PREPRINT

tascc

TASCC-P-95-28

ELASTIC RECOIL DETECTION (ERD) WITH EXTREMELY HEAVY IONS

J.S. Forster
AECL, Chalk River Laboratories, Chalk River, Ontario K0J 1J0, Canada

P.J. Currie
Royal Tyrrell Museum, Drumheller, Alberta T0J 0Y0, Canada

J.A. Davies, R. Siegele and S.G. Wallace
Accelerator Laboratory, McMaster University,
Hamilton, Ontario L8S 4M1, Canada

D. Zelenitsky
Department of Geology and Geophysics, University of Calgary,
Calgary, Alberta T2N 1N4, Canada

Submitted to
Nucl. Instr. and Meth. B

NOTICE

This report is not a formal publication; if it is cited as a reference, the citation should indicate that the report is unpublished. To request copies our E-Mail address is **TASCC@CRL.AECL.CA.**

Physical and Environmental Sciences
Chalk River Laboratories
Chalk River, ON K0J 1J0 Canada

1995 August

Elastic Recoil Detection (ERD) with Extremely Heavy Ions

J.S. Forster
AECL, Chalk River Laboratories, Chalk River, Ontario, Canada K0J 1J0

P.J. Currie
Royal Tyrrell Museum, Drumheller, Alberta, Canada T0J 0Y0

J.A. Davies, R. Siegele and S.G. Wallace
Accelerator Laboratory, McMaster University,Hamilton, Ontario, Canada L8S 4M1

D. Zelenitsky
Department of Geology and Geophysics, University of Calgary, Calgary, Canada T2N 1N4

Abstract

Extremely heavy ion beams such as ^{209}Bi in elastic recoil detection (ERD) makes ERD a uniquely valuable technique for thin-film analysis of elements with mass $\leq$ 100. We report ERD measurements of compositional analysis of dinosaur eggshells and bones. We also show the capability of the ERD technique on studies of thin film, high temperature superconductors.

INTRODUCTION

Rutherford backscattering spectrometry (RBS) with light ions has long been used for measuring depth profiles of elements in the near-surface region of solids [1]. The major limitations in RBS are the poor mass resolution for heavy elements and low sensitivity for light elements. In contrast, elastic recoil detection (ERD) allows unambiguous identification of and a high sensitivity to all elements from hydrogen to elements with masses approaching the mass of the beam.

The pioneering work of L'Ecuyer et al. [2] used 20 - 30 MeV beams of ^{32}S and ^{35}Cl to measure low-Z surface impurities such as H,D,Li,C and O in heavier substrates. Later work by Doyle and Peercy [3] showed that H and D could be measured by ERD using low-energy (1 - 3 MeV) beams of ^{4}He.

ERD becomes an even more valuable ion-beam analysis method with very heavy-ion beams as demonstrated by Stoquert et al. [4] where beams of ^{127}I, up to 240 MeV, were used. This results from consideration of the kinematics when a monoenergetic beam of ions of mass M_1 bombards a target of mass M_2. The energy of the recoils E_2 is given by:

$$E_2 = 4\, M_1M_2/(M_1+M_2)^2\, E_1\, \cos^2\theta \qquad (1)$$

where θ is the angle of the beam to the detector and E_1 is the energy of the beam. When $M_1 \gg M_2$ this can be rewritten as:

$$E_2/M_2 \approx 4E_1/M_1\, \cos^2\theta \qquad (2)$$

and, hence, all recoils have similar velocities.

The cross section for ERD is given by:

$$\sigma_{ERD} = (Z_1/Z_2e^2/2E_1)^2 ((M_1+M_2)/M_2)^2 \cos^{-3}\theta \quad (3)$$

which for $M_1 \gg M_2$ approximates to:

$$\sigma_{ERD} = (Z_1M_1e^2/2E_1)^2 (Z_2/M_2)^2 \cos^{-3}\theta \quad (4)$$

Since $Z_2/M_2 \sim 0.4 - 0.5$, the sensitivity is approximately the same for all elements. Also, the cross section scales as Z_1^4.

A further advantage of heavy-ion beams comes from the calculation of the maximum scattering angle of the incident beam which is:

$$\theta_{max} = \sin^{-1}(M_2/M_1) \quad (5)$$

so that, in most cases, beam particles are not scattered into the detector.

We have used the heavy-ion ERD technique, with beams of 230 MeV ^{209}Bi ions, to profile light elements in the near-surface region of dinosaur bones and eggshell fragments. The purpose of the experiment was to determine if these fragments, which come from widely-separated dinosaur beds, would show different elemental composition during fossilization. We also show results for ERD analysis of thin-film high Tc materials

EXPERIMENT

A beam of 230 MeV ^{209}Bi ions was obtained from the tandem accelerator of the TASCC (tandem accelerator superconducting cyclotron) facility at Chalk River. The samples were mounted on a two-axis goniometer with x- and y-translation; this allowed us to mount up to 9 samples at a time. The target was set at 35° to the beam direction and recoiling atoms were detected in a large

solid angle ionization detector positioned at 45° to the beam

The detector is very similar to the one described by Assmann et al. [5,6]. It consists of a cathode, Frisch grid and anode which are all 6 cm. wide and 30 cm. long; the distance from the cathode to the grid is 5 cm. and from the grid to the anode is 1 cm. The cathode is divided into two insulated "backgammon" shapes and charges induced in the right (r) and left (l) sides allow a determination of the x-coordinate of the detected particle by $x = (l-r)/(l+r)$. Since the charge induced at the cathode is proportional to the total energy E of the ionizing particle and its distance from the Frisch grid we can determine the y-coordinate by $y = (l+r)/E$. Thus we can kinematically compensate the total energy signal to a common angle since the detector subtends ± 1.6° in the vertical and horizontal directions.

The anode is subdivided into three regions of length 3 cm. (ΔE_1), 9 cm. (ΔE_2) and 18 cm.(E_R). In normal operation we use the sum of ΔE_1 and ΔE_2 as the ΔE signal. However, for very heavy recoils e.g. $M_2 > 60$, we plot ΔE_1 versus ($\Delta E_2 + E_R$) for particle identification because of the shorter range of heavier recoils.

Isobutane, at a pressure of 30 Torr, was used in all of the measurements presented here with voltages of cathode to Frisch grid of 150 V and grid to anode of 150 V i.e. E/p = 1 V/cm-Torr between cathode and grid. The active gas volume is surrounded on both sides and back by wires connected to a voltage divider chain to provide a uniform field between cathode and grid. The detector window is a 70 $\mu m/cm^2$ stretched polyethylene foil supported by a 92% transmission

stainless steel grid and subtends a solid angle of 5 msr. Finally, a 300 mm^2, 300 μm thick silicon surface barrier detector is situated behind the field wires at the rear of the detector. The silicon detector is used to detect recoils lighter than boron since these give only small signals in the gas detector.

RESULTS

A plot of ΔE ($\Delta E_1 + \Delta E_2$) versus E_R is shown in figure 1a for bombardment of an extinct ostrich eggshell from the Gobi desert and in figure 1b for a dinosaur eggshell fragment. Both samples had been lapped to remove the surface layer and expose the inner section of the eggshell. Figure 1 clearly shows that there is little difference between the two samples which was confirmed by detailed analysis of the data. Figure 2 illustrates kinematically corrected energy spectra of the major components in the dinosaur eggshell.

Figure 3 shows ΔE versus E_R plots for dinosaur bone fragments (a centrosauros skull fragment and a pachyrhinosauroas coracoid fragment) taken from two widely-separated dinosaur beds. It is clear that there are differences in the two spectra and the differences are more clearly revealed in Table 1 where the composition of the two bone fragments is given. The main components of the bones (C,O,P and Ca) are similar, as would be expected, whereas there are major differences in the other elements, most notably Al, Si and Fe which would have been taken up during fossilization.

Finally, figure 4 shows plots of ΔE_1 versus $(\Delta E_2 + E_R)$, and ΔE $(\Delta E_1 + \Delta E_2)$ versus E_R for a thin film of $YBa_2Cu_3O_{7-x}$ superconductor on a $LaAlO_3$ substrate. The plot of ΔE versus E_R in Figure 4a shows that we clearly separate elements up to Cu but the heavier masses are not easily resolved. Figure 4b, on the other hand, showing ΔE_1 versus $(\Delta E_2 + E_R)$ shows that we can easily distinguish between Cu, Y and Ba/La.

CONCLUSIONS

The use of high-energy (1 - 2 AMeV) beams of very heavy ions provides a semi-universal technique for measuring elemental composition of materials in the near-surface region. Since the cross section scales as Z_1^4 very low beam doses are required to achieve sensitivities below 10^{14} atoms/cm^2.

By using a subdivided anode in our ionization chamber we have shown that we can easily resolve all elements up to at least M_1 /2. In particular, this detector has proven very useful in studies of thin-film high Tc material.

Finally, the position sensitivity of the detector allows us to use a large solid angle with kinematic correction.

REFERENCES

1. WK. Chu, J.W. Mayer and M.A. Nicolet, Backscattering Spectrometry (Academic Press, New York, 1978).

2. J L'Ecuyer, C. Brassard, C. Cardinal and B. Terrault, Nucl. Instr. and Meth. 149(1978)271.

3. B.L. Doyle and R.S. Peercy, Appl. Phys. Lett. 34(1979)811.

4. J.P. Stoquert, G. Guillaume, M. Hage-Ali, J.J. Grob, C. Ganter and P. Siffert, Nucl. Instr. and Meth. B44(1989)184.

5. W. Assmann, P. Hartung, H. Huber, P. Staat, H. Steffens and Ch. Steinhausen, Nucl. Instr. and Meth. B85(1994)726.

6. W. Assmann, H. Huber, Ch. Steinhausen, M. Dobler, H. Glückler and A. Weidinger, Nucl. Instr. and Meth. B89(1994)131.

TABLE 1

Composition of Dinosaur Bone Fragments from Two Widely Separated Dinosaur Beds

Element	Fragment (%)	Fragment 2 (%)
C	9.5	9.4
N	0.3	0.2
O	58.8	56.3
F	4.1	6.0
Na	0.7	1.1
Mg	0.2	0.2
Al	1.8	0.5
Si	1.3	0.8
P	8.5	8.9
Ca	14.0	14.5
Fe	0.8	2.1

FIGURE CAPTIONS

Figure 1 (a)ΔE versus E_R plots for recoils from a modern ostrich eggshell from the Gobi desert.

(b) same as (a) but for a dinosaur eggshell fragment.

Figure 2 Kinematically corrected total energy spectra for the major elements (C,O and Ca) in figure 1a.

Figure 3 ΔE versus E_R plots for recoils from two dinosaur bone fragments coming from two widely separated dinosaur beds. The major components (C,O,P and Ca) have similar intensities whereas there are differences in the other components (see Table 1).

Figure 4 (a) Plot of ΔE versus E_R for a thin film of $YBa_2Cu_3O_{7-x}$ on a thick $LaAlO_3$ substrate.

(b) same as (a) but for ΔE_1 versus $(\Delta E_2 + E_R)$.

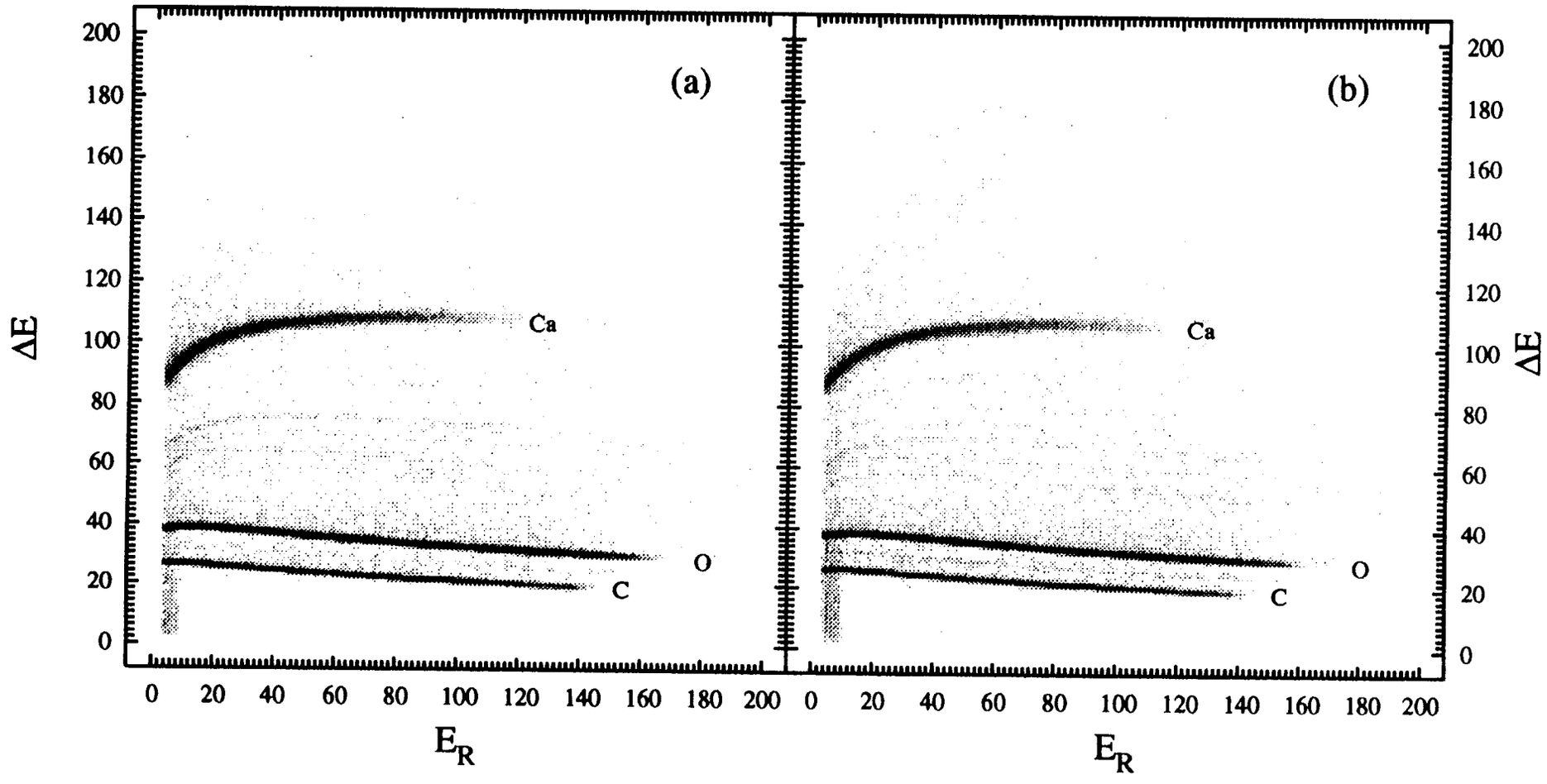
(a)
(b)
Ca
O
C
ΔE
E_R
0
20
40
60
80
100
120
140
160
180
200

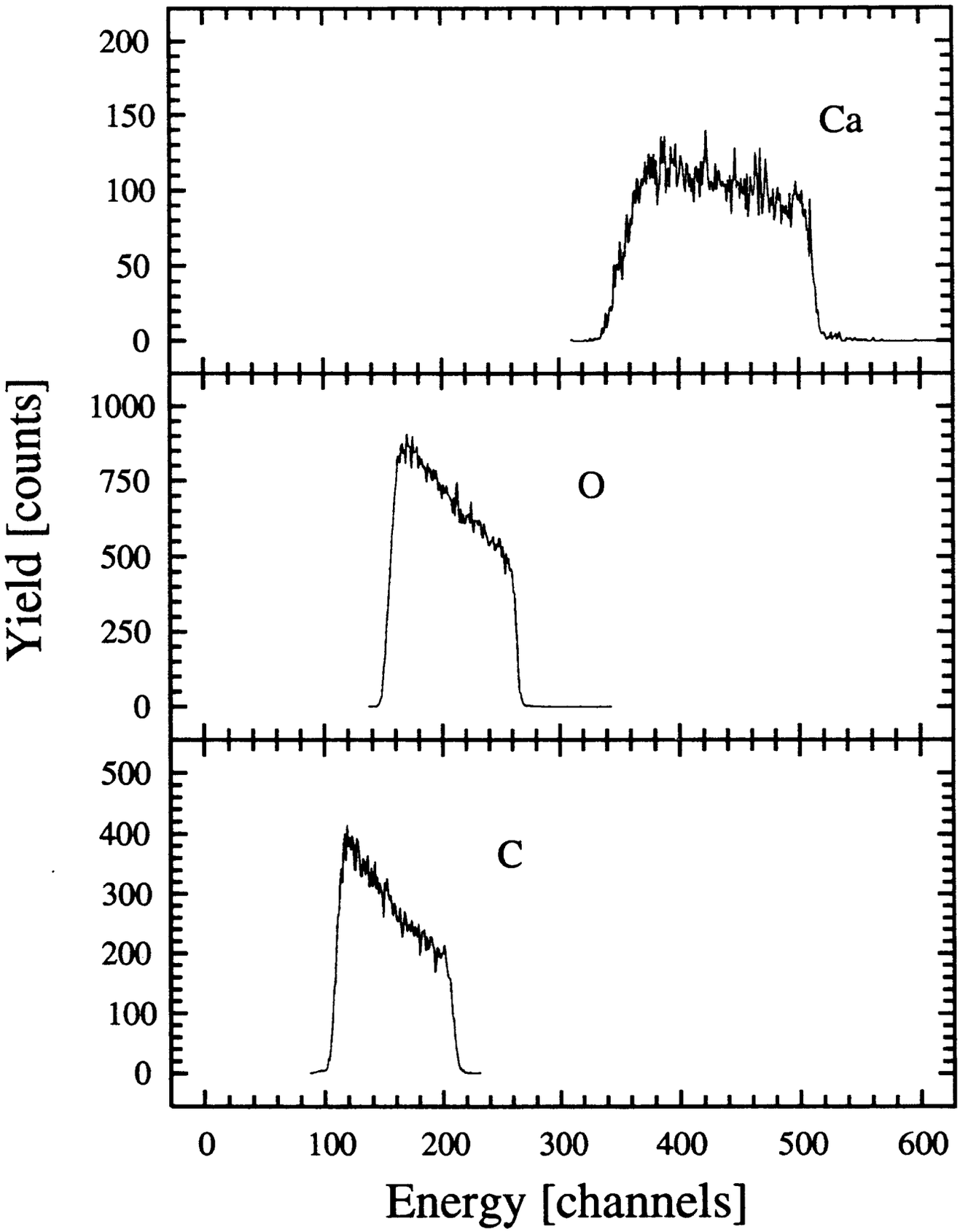
Yield [counts]
200
150
100
50
0
Ca
1000
750
500
250
0
O
500
400
300
200
100
0
C
0
100
200
300
400
500
600
Energy [channels]

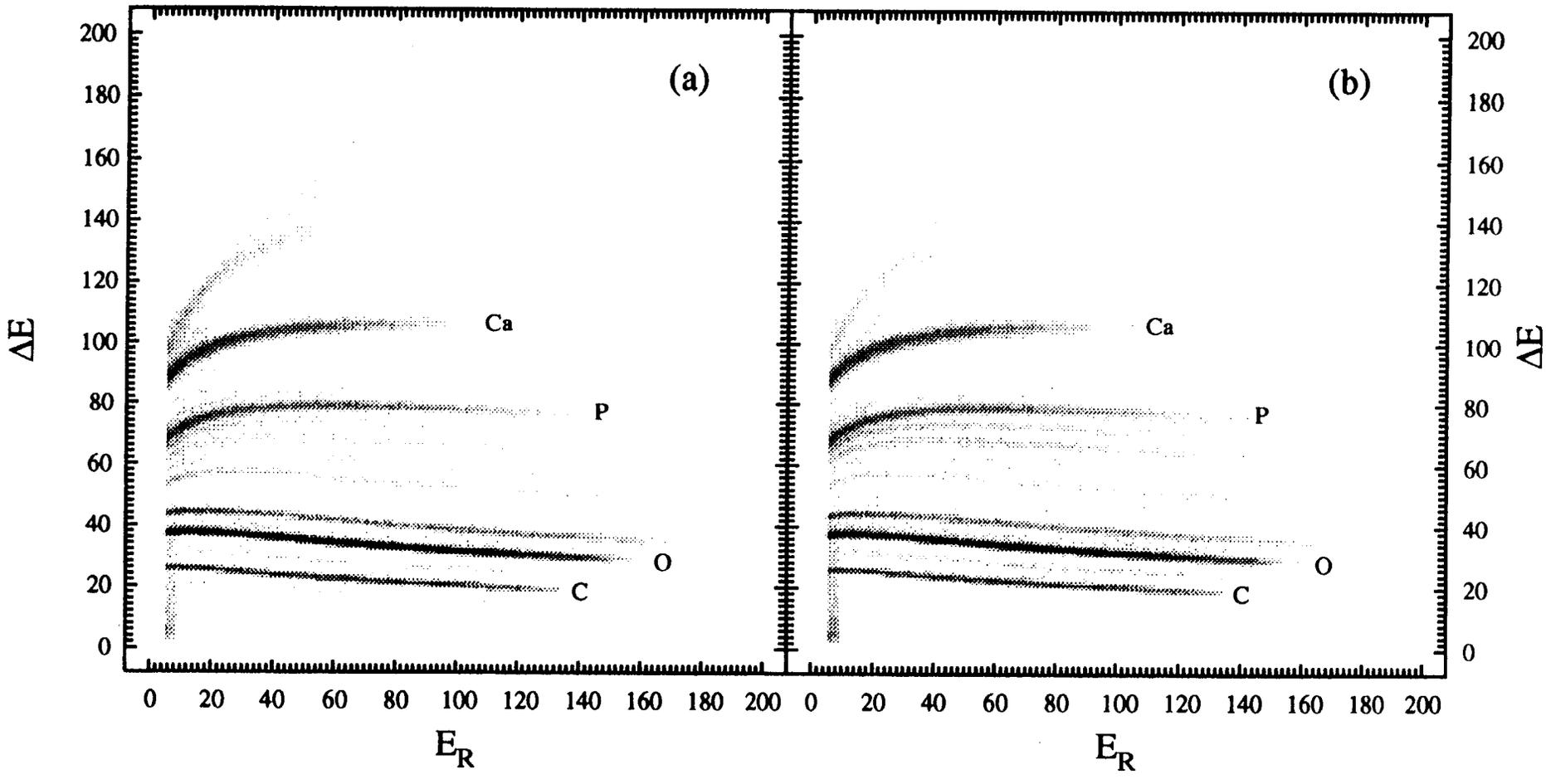

Fig. 3

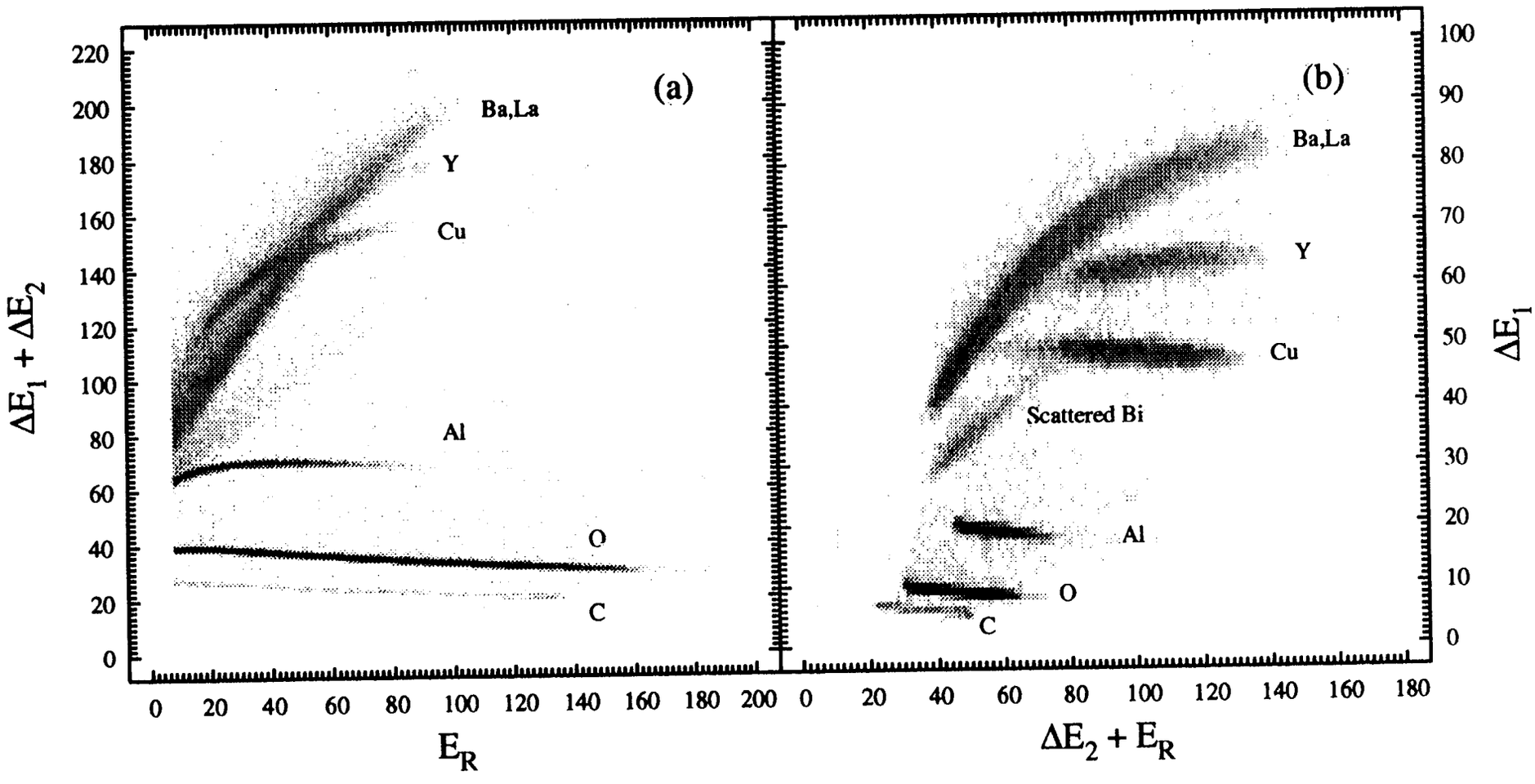
(a)
Ba,La
Y
Cu
Al
O
C
$\Delta E_1 + \Delta E_2$
E_R
0 20 40 60 80 100 120 140 160 180 200
0 20 40 60 80 100 120 140 160 180 200 220
(b)
Ba,La
Y
Cu
Scattered Bi
Al
O
C
$\Delta E_2 + E_R$
ΔE_1
0 10 20 30 40 50 60 70 80 90 100